Role of GPR52 in the regulation of lipogenesis in liver

（肝臓のGPR52の脂質合成制御における役割）

千葉大学大学院医学薬学府

先端医学薬学専攻

（主任：三木　隆司教授）

和田　光生

SUMMARY

Gpr52 is an orphan G-protein-coupled receptor of unknown physiological function. We found that Gpr52-deficient ($Gpr52^{-/-}$) mice exhibit leanness associated with reduced liver weight, decreased hepatic *de novo* lipogenesis, and enhanced insulin sensitivity. Treatment of the hepatoma cell line HepG2 cells with c11, the synthetic GPR52 agonist, increased fatty acid biosynthesis, and GPR52-knockdown (KD) abolished the lipogenic action of c11. In addition, c11 induced expressions of lipogenic enzymes (*SCD1* and *ELOVL6*), while these inductions were attenuated by GPR52-KD. In contrast, cholesterol biosynthesis was not increased by c11, but its basal level was significantly suppressed by GPR52-KD. High-fat diet (HFD)-induced increase in hepatic expression of *Pparg2* and its targets (*Scd1* and *Elovl6*) was absent in $Gpr52^{-/-}$ mice with alleviated hepatosteatosis. Our present study showed that hepatic GPR52 promotes biosynthesis of fatty acid and cholesterol in a ligand-dependent and a constitutive manner, respectively, and Gpr52 participates in HFD-induced fatty acid synthesis in liver.

Keywords: GPR52, PPARγ2, SCD1, ELOVL6, fatty acid biosynthesis, hepatosteatosis

INTRODUCTION

G-protein-coupled receptors (GPCRs) comprise numerous receptor proteins on the plasma membrane that share the common structural feature of having seven transmembrane domains (Gusach et al., 2020; Hilger et al., 2018; Ritter and Hall, 2009; Wootten et al., 2018). GPCRs are known to regulate various cellular functions by coupling with intracellular partners including canonical transducer proteins (i.e., heterotrimeric GTP-binding proteins) and scaffolding proteins (e.g., arrestins, PDZ scaffolds, and non-PDZ scaffolds) (Wootten et al., 2018). Structurally and evolutionarily, GPCRs are classified into several subfamilies including class A (rhodopsin-like), class B1 (secretin receptor-like), class B2 (adhesion receptors), class C (metabotropic glutamate receptor-like), and class F (frizzled- like) subfamilies.

In humans, more than 800 GPCR genes have been identified, and a variety of molecules have been found to act as their ligands. These include hormones, neurotransmitters, ions, photons, odorants, and fatty acids; binding of each ligand to its corresponding GPCR evokes unique GPCR signaling. However, specific ligands have not been identified for many GPCRs; such GPCRs are known as orphan GPCRs (Wootten et al., 2018). GPR52 is one such class-A orphan GPCR, which constitutively activates adenylyl cyclase without inhibiting forskolin-stimulated cAMP elevation, as is the case with GPR3, GPR21, and

GPR65 (Martin et al., 2015). Precise analysis of its expression pattern in the brain revealed that GPR52 is abundantly expressed in striatum, where it is co-localized with dopamine D1 (DRD1) and/or D2 (DRD2) receptors (Komatsu et al., 2014). hGPR52-expressing transgenic mice exhibit decreased methamphetamine-induced hyperlocomotion, while Gpr52 knockout mice ($Gpr52^{-/-}$ mice) exhibit psychosis-related behaviors, suggesting that GPR52 is involved in modulating cognitive function and emotion through dopamine signaling (Komatsu et al., 2014).

To clarify the physiological role of Gpr52, we generated $Gpr52^{-/-}$ mice, and found that $Gpr52^{-/-}$ mice weighed less and showed reduced fat and liver weight, suggesting that Gpr52 involvement in the regulation of energy metabolism. $Gpr52^{-/-}$ mice also showed increased insulin sensitivity as assessed by insulin-induced Akt phosphorylation. As these knockout mice exhibited neither hyperlocomotion nor hypophagia, involvement of Gpr52 expressed in tissues other than the brain was implicated. To ascertain its relevance, we examined the tissue expression pattern of GPR52 in human cDNAs; unexpectedly, considerable GPR52 expression was noted in liver. Functional analyses of GPR52 using $Gpr52^{-/-}$ liver and GPR52-knocked down HepG2 cells revealed that hepatocyte GPR52 regulates biosynthesis of fatty acid in the liver and contributes to the acceleration of hepatosteatosis in response to excessive fat intake in mice.

RESULTS

Gpr52^{-/-} Mice Exhibit Reduced Adiposity

To clarify the physiological role of GPR52, we generated *Gpr52^{-/-}* mice (Figure S1A).

Although these mice display no gross physical abnormalities and are fertile, their body

weight was significantly less than that of wild-type (WT) mice. *Gpr52^{-/-}* mice showed

reduced adiposity manifested in reduced body weight and the reduced tissue weight of

inguinal white adipose tissue (ingWAT), epididymal WAT (epiWAT), and brown adipose

tissue (BAT) together with unchanged body length (Figure 1A, 1B, and S1B). In addition,

liver weight was significantly reduced in *Gpr52^{-/-}* mice. Since food intake and locomotor

activity (Figure S1C and S1D) did not differ between *Gpr52^{-/-}* and WT mice, the leanness

of *Gpr52^{-/-}* mice is unlikely to be due to the decreased energy intake and/or the increased

energy consumption associated with hyper-locomotive activity.

Gpr52^{-/-} Mice Exhibit Enhanced Insulin Sensitivity

As *Gpr52^{-/-}* mice show significantly decreased tissue weight of adipose tissues and liver,

two principal insulin target tissues, we evaluated their insulin sensitivity. Although there

was no significant difference in blood glucose levels under *ad lib* fed conditions, plasma

insulin levels tended to be lower ($p = 0.052$) in *Gpr52^{-/-}* mice (Figure S1E). Insulin

sensitivity assessed by insulin tolerance test showed that the glucose lowering effect of exogenous insulin tended to be greater in $Gpr52^{-/-}$ mice (Figure S1F). Oral glucose tolerance test (OGTT) revealed that $Gpr52^{-/-}$ mice have normal glucose tolerance with significantly reduced insulin secretory response to glucose (Figure 1C), suggesting that $Gpr52^{-/-}$ mice have enhanced insulin sensitivity.

We then evaluated the insulin sensitivity of adipose tissue and liver of $Gpr52^{-/-}$ mice *in vivo* by quantifying Akt phosphorylation in response to exogenous insulin administration. Intravenous administration of insulin induced a significant increase in phosphorylated Akt (p-Akt) levels in epiWAT and liver of both $Gpr52^{-/-}$ and WT mice. However, the p-Akt/Akt ratio in these tissues after insulin treatment was significantly higher in $Gpr52^{-/-}$ mice than that in WT mice (Figure 1D), indicating that insulin sensitivity is enhanced in $Gpr52^{-/-}$ mice.

GPR52 Is Expressed in Adipose Tissue and Liver in Humans and Mice

The lack of hypophagia or hyperlocomotion in $Gpr52^{-/-}$ mice suggested that their leanness may be attributable to dysfunction of Gpr52 expressed in tissues other than brain. We therefore examined the tissue expression profile of $GPR52$ in humans (Figure 2A). As previously reported, $GPR52$ was found to be highly expressed in human brain, but was

also expressed in liver (Figure 2A). In addition, *GPR52* mRNA was expressed in the human hepatoma cell line HepG2 cells at a level similar to that in human liver, demonstrating that GPR52 is expressed in hepatocytes. In mouse tissues, *Gpr52* was substantially expressed in adipose tissues and liver (Figure 2B). qPCR experiment using mature adipocytes and stromal vascular fraction (SVF) isolated from epiWAT revealed that Gpr52 was expressed in mature adipocytes (Figure 2C). Based on these results, we hypothesized that Gpr52 expressed in adipocytes and/or hepatocytes plays a role in lipid metabolism.

Gene Expressions of the Enzymes Involved in Biosynthesis of Fatty Acid and Cholesterol Were Altered in epiWAT and Liver of *Gpr52*^{-/-} Mice

As fat depots and liver of $Gpr52^{-/-}$ mice weighed significantly less than those of WT mice, we hypothesized that *de novo* fatty acid synthesis in adipose tissues and/or liver might be decreased. We therefore quantified the mRNA expressions of genes involved in *de novo* lipid synthesis in ingWAT, epiWAT, BAT, and liver (Figure 2D). Contrary to our expectation, mRNA expressions of *Scd1*, *Elovl6*, and *Acc1* of $Gpr52^{-/-}$ mice were not decreased in ingWAT, BAT, or liver, despite the lesser weight of these tissues in $Gpr52^{-/-}$ mice. Nevertheless, mRNA expressions of *Scd1*, *Elovl6*, and *Acc1* of $Gpr52^{-/-}$ mice were

significantly reduced in epiWAT. Among many *de novo* lipogenic enzymes, Scd1 (Dobrzyn et al., 2010), Elovl6 (Shimano, 2012), and Acc1 (Kim et al., 2017) have been reported to play critical roles in the regulation of fatty acid metabolism, suggesting that Gpr52 may be involved in the regulation of fatty acid biosynthesis.

Unexpectedly, mRNA expression of *Hmgcr*, the rate-limiting enzyme of cholesterol biosynthesis, was significantly decreased in *Gpr52*$^{-/-}$ liver. In addition, similar to the changes of *Scd1*, *Elovl6*, and *Acc1* expressions, *Hmgcr* expression was significantly reduced in epiWAT, but not in ingWAT or BAT. These results suggest that Gpr52 may also participate in the regulation of cholesterol biosynthesis as well as that of fatty acid.

Gpr52 Is Involved in *Ex vivo* Synthesis of Fatty Acid and Cholesterol in epiWAT and Liver

Alteration of gene expressions of the enzymes of *de novo* synthesis of fatty acid and cholesterol in *Gpr52*$^{-/-}$ epiWAT and liver led us to examine their *de novo* synthesis *ex vivo* using ^{14}C-acetate in organ culture (Figure 3A and 3B). In accord with the changes in mRNA expressions, *de novo* lipid synthesis of *Gpr52*$^{-/-}$ epiWAT tended to be low for fatty acid and was significantly reduced for cholesterol, when compared with those of WT epiWAT (p = 0.037). In addition, *de novo* lipid synthesis in liver of *Gpr52*$^{-/-}$ mice showed

8

a similar tendency; *de novo* synthesis of both fatty acid (statistically insignificant) and

cholesterol (p = 0.013) was decreased in *Gpr52*^{-/-} mice. These results are compatible with

our thesis that Gpr52 expressed in adipocytes and hepatocytes is involved in *de novo*

synthesis of fatty acid and cholesterol.

GPR52 Expressed in HepG2 Cells Promotes Fatty Acid and Cholesterol Biosynthesis

in a Ligand-dependent- and Constitutive-manner, Respectively

Since GPR52 was expressed in HepG2 cells (Figure 2A), we elucidated the regulatory

mechanism of *de novo* lipid synthesis by GPR52 using this cell line. In addition, we

utilized the GPR52 agonist c11, which was established by Takeda Pharmaceutical

Company Limited as a specific agonist of GPR52 (Nakahata et al., 2018).

   We first evaluated the pharmacological characteristics of c11. We transfected HEK293

cells with either vehicle, GPR52 or GPR21. GPR21 is another orphan GPCR, which has

the highest structural similarity to GPR52, and may have functional similarity to GPR52,

since Gpr21 is expressed abundantly in the brain and its genetic disruption evokes

leanness and enhanced insulin sensitivity in mice (Osborn et al., 2012). In accord with a

previous report indicating that both GPR52 and GPR21 are constitutively active GPCRs

(Martin et al., 2015), overexpression of either GPR52 or GPR21 was found to

significantly upregulate the intracellular cAMP concentrations ([cAMP]$_i$) (Figure S2B).

Treatment of the cells with a higher concentration of c11 further increased the [cAMP]$_i$

levels in a dose-dependent manner in GPR52-expressing cells, but not in vehicle-

transfected cells or in GPR21-expressing cells, supporting the previous report that c11 is

a specific agonist of GPR52 (Figure S2A and S2B).

We then examined the effect of c11 on [cAMP]$_i$ in HepG2 cells treated with GPR52-

siRNA (GPR52-KD HepG2) or control-siRNA (Cont-HepG2) (Figure 3C, S2C). We

found that c11 treatment increased [cAMP]$_i$ in Cont-HepG2, but that the response was

attenuated in GPR52-KD HepG2, suggesting that the endogenous GPR52 is functional in

the HepG2 cells.

In addition, GPR52-KD HepG2 and Cont-HepG2 were subjected to measurement of

de novo lipogenesis using ^{14}C-acetate (Figure 3D-3F). As with *de novo* fatty acid

synthesis, c11 dose-dependently increased such synthesis in Cont-HepG2 cells (Figure

3E). Although GPR52 knockdown did not affect its basal rate, c11-dependent increase in

fatty acid synthesis was abolished in GPR52-KD HepG2 cells. In contrast, *de novo*

cholesterol synthesis in Cont-HepG2 cells was not increased by c11; however, the basal

rate was significantly suppressed by GPR52 knockdown (Figure 3F). These results

suggest that hepatic GPR52 ligand-dependently promotes fatty acid biosynthesis and

constitutively upregulates cholesterol biosynthesis.

To clarify the mechanism of GPR52 action on lipid biosynthesis, we examined gene expression changes due to GPR52 knockdown in HepG2 cells (Figure 3G). We first quantified the expressions of *SCD1* and *ELOVL6*, the genes for the two critical enzymes involved in regulation of fatty acid metabolism. Interestingly, their expressions were increased by c11 in a dose-dependent manner in Cont-HepG2 cells, while the effect of c11 was significantly attenuated in GPR52-KD HepG2 cells. The trend of the changes of *SCD1* and *ELOVL6* expressions was compatible with that of *de novo* fatty acid synthesis in HepG2 cells. Taken together, these results indicate that ligand-dependent activation of GPR52 promotes *de novo* fatty acid synthesis at least in part through transactivating *SCD1* and *ELOVL6*.

We also examined the expression of *HMGCR*, the gene for the rate-limiting enzyme of cholesterol biosynthesis (Figure 3G). In contrast to the lack of effect of c11 on *de novo* cholesterol synthesis in Cont-HepG2 cells, c11 dose-dependently increased *HMGCR* expression, which was diminished in GPR52-KD HepG2 cells. Nevertheless, knockdown of GPR52 significantly decreased *HMGCR* expression. These results suggest that *HMGCR* expression is regulated by ligand-stimulation of GPR52 as well as by the basal expression level of GPR52; the total rate of cholesterol biosynthesis may therefore be

determined by enzymes other than HMGCR.

GPR52 Accelerates Fat Accumulation in Liver and Induces Insulin Resistance in Response to Excessive Fat Intake

Gpr52⁻ᐟ⁻ mice exhibited enhancement of insulin sensitivity and reduction of tissue weight and *de novo* lipogenic gene (*Scd1, Elovl6,* and *Acc1*) expressions in epiWAT. As Scd1 and Elovl6 are key regulators of lipid metabolism, we hypothesized that *Gpr52⁻ᐟ⁻* mice may have defective triglyceride accumulation in liver when exposed to excessive fat intake. We therefore treated *Gpr52⁻ᐟ⁻* mice with high fat diet (HFD) and examined levels of lipid metabolism and insulin sensitivity. Although *Gpr52⁻ᐟ⁻* mice weighed less under normal chow diet, their HFD-induced body weight gain (18.3% after 10-week-HFD feeding) was similar to that of WT mice (23.7%) as estimated by the relative increase by HFD feeding, suggesting that *Gpr52⁻ᐟ⁻* mice retain the capacity for developing diet-induced obesity (Figure 4A). However, the HFD-induced increase in fasting plasma insulin levels was significantly ($p = 0.00012$) less in *Gpr52⁻ᐟ⁻* mice than that in WT mice (Figure 4B), suggesting that *Gpr52⁻ᐟ⁻* mice are partially protected from diet-induced insulin resistance. Although plasma glucose levels during OGTT were only modestly lower in *Gpr52⁻ᐟ⁻* mice, their plasma insulin levels were significantly lower (Figure 4C), suggesting that insulin

sensitivity was enhanced in *Gpr52-/-* mice under HFD. In addition, considering that Gpr52

is shown to be expressed also in pancreatic islets (Figure 2B), decreased insulin secretion

in *Gpr52-/-* mice during OGTT might well reflect altered insulin secretion from pancreatic

β cells. HFD feeding induced a significant increase in liver weight in both *Gpr52-/-* and

WT mice; however, the liver weight was significantly (p = 0.0009) lower in *Gpr52-/-* mice

than that in WT mice (Figure 4D). Under normal diet conditions, triglyceride content in

liver was not statistically different between *Gpr52-/-* and WT mice (Figure 4D). However,

under HFD feeding, the triglyceride content in *Gpr52-/-* liver was moderately, but

significantly (p = 0.0001) lower than that in WT, suggesting that Gpr52 is involved in the

development of diet-induced hepatosteatosis.

We then examined the gene expressions of *Scd1*, *Elovl6*, *Acc1,* and *Acc2* in *Gpr52-/-*

liver. Interestingly, mRNA expressions of *Scd1* and *Elovl6* were significantly increased

by HFD-feeding in WT liver (Figure 4E), in accord with the previous reports (Chan et al.,

2008; Hu et al., 2004; Oosterveer et al., 2009); however, the increase by HFD feeding

was completely abolished in *Gpr52-/-* liver. Furthermore, HFD feeding did not increase

Acc1 expression in WT liver, but rather suppressed it in *Gpr52-/-* liver. *Acc2* expression

tended to be increased by HFD in WT mice, but not in *Gpr52-/-* mice.

We then investigated the molecular mechanisms involved in the changes of *Scd1* and

13

Elovl6 expressions by HFD feeding by comparing mRNA expressions of *Srebp1c* and *Pparg2* in *Gpr52^{-/-}* and WT liver (Figure 4E). Hepatic *Srebp1c* expression of *Gpr52^{-/-}* mice was not different from that of WT mice. Interestingly, mRNA expression of *Pparg2* was significantly increased by HFD feeding in WT liver, but not in *Gpr52^{-/-}* liver, suggesting that Gpr52 is critical in HFD-induced *Pparg2* upregulation in the liver.

DISCUSSION

GPR52 is an orphan GPCR that couples with the stimulatory G protein Gs (Allen et al. 2017; Komatsu et al., 2014). When expressed in cells, GPR52 activates Gs signaling and increases $[cAMP]_i$ in the absence of its ligand (Martin et al., 2015). Recently, Lin *et al.* clarified the molecular structure and the mode of constitutive activity of GPR52 using crystal structure analysis (Lin et al., 2020). They found that extracellular loop 2 (ECL2) of GPR52 occupies the orthosteric ligand-binding pocket, which contributes to its self-activation. In addition, they identified the surrogate agonist c17, and showed that GPR52 has a very high level of basal activation that reaches as high as 90% of the maximal activation induced by c17.

In contrast, Setoh *et al.* identified another GPR52 agonist, compound 7m, and found that it dose-dependently increased $[cAMP]_i$ concentrations in CHO cells expressing

GPR52 (Setoh et al., 2014). The cAMP-increasing effect of c11 in HEK293 cells expressing GPR52 in our present study was consistent with the result by Setoh *et al*. In addition, recent studies found that 3-BTBZ, another agonist of GPR52, potently increased $[cAMP]_i$ in a β-arrestin 2-independent manner in frontal cortical neurons (Hatzipantelis et al., 2020).

Interestingly, fatty acid biosynthesis was dose-dependently increased by c11 in HepG2 cells, which effect was absent in GPR52-KD HepG2 cells. These results indicate that fatty acid biosynthesis can be further upregulated by GPR52 activation. In contrast, cholesterol biosynthesis was not increased by c11 in HepG2 cells, while it was significantly reduced by GPR52 knockdown, suggesting that GPR52 is critical in the regulation of cholesterol biosynthesis in liver. In addition, mRNA expression of *Hmgcr* was significantly decreased in epiWAT and liver of $Gpr52^{-/-}$ mice. The activity of Hmgcr is known to be regulated both transcriptionally (Luo et al., 2020; Tian et al., 2010) and post-transcriptionally (van den Boomen et al., 2020; Khan et al., 2020), implying that decreased *Hmgcr* expression in epiWAT and liver of $Gpr52^{-/-}$ mice might well contribute to the reduction of *de novo* cholesterol biosynthesis seen in these tissues. The lack of effect of c11 may suggest that self-activation of GPR52 is sufficient for full activation of cholesterol biosynthesis. Alternatively, cAMP has been shown to activate phosphoprotein phosphatase inhibitor-1

(PPI-1), resulting in the decrease of cholesterol biosynthesis through inactivation of HMGCR (Bathaie et al., 2017). In addition, Hu *et al.* reported that prenatal caffeine exposure (PCE) increased hepatic expression of *Hmgcr* via lowering hepatic cAMP concentrations (Hu et al., 2019). By contrast, cAMP/PKA/CREB signaling has been reported to upregulate hepatic HMGCR expression (Tian et al., 2010). Therefore, it is still unclear whether or not decreased cAMP contributes to the decrease in cholesterol biosynthesis noted in our GPR52 knockdown HepG2 cells.

We further elucidated the molecular mechanism of GPR52-dependent biosynthesis of fatty acid and found that the gene expressions of *SCD1* and *ELOVL6* were induced by GPR52-activation by c11. These genes have been shown to play a critical role in fatty acid metabolism in liver. Stearoyl-CoA desaturase-1 (SCD1) is the rate-limiting enzyme of monounsaturated fatty acids (MUFAs) formation (ALJohani et al., 2017; Dobrzyn et al., 2010). Elongation of very long chain fatty acids protein 6 (ELOVL6) is an enzyme that lengthens saturated and monounsaturated fatty acids with 12, 14, and 16 carbons (Guillou et al., 2010; Shimano, 2012). In addition, we found that hepatic expression *Acc1* in *Gpr52$^{-/-}$* mice tended to be lower (p = 0.053) than in WT mice only under HFD feeding. Acetyl-CoA carboxylase 1 (ACC1) is a rate-limiting enzyme of biosynthesis of fatty acids that catalyzes carboxylation of acetyl-CoA to produce malonyl-CoA (Kim et al., 2017;

Wakil and Abu-Elheiga, 2009). When fed HFD, Elovl6-deficient mice develop obesity

and hepatosteatosis, but remain insulin sensitive (Matsuzaka et al., 2007). By contrast,

Scd1-deficient mice are resistant to obesity, hepatosteatosis, and insulin resistance in

response to HFD feeding (Ntambi et al., 2002). Moreover, liver-specific Acc1-deficient

mice are protected from HFD-induced hepatosteatosis (Mao et al., 2006). Considering

these results together, the lack of increase in hepatic *Scd1* expression by HFD may play a

role in protecting *Gpr52*^{-/-} mice from developing hepatosteatosis under HFD.

We also investigated the molecular mechanisms of the changes in *Scd1* and *Elovl6*

expressions by HFD feeding. Transcriptional regulation of *Scd1* and *Elovl6* has been

studied intensively, and they were reported to be transactivated by SREBP1c (Mauvoisin

and Mounier, 2011) and PPARγ (Morán-Salvador et al., 2011). Interestingly, we found

that hepatic expression of *Pparg2* was significantly increased in WT mice, but not in

Gpr52^{-/-} mice (Figure 4E). HFD feeding of mice has been reported to upregulate *Pparg2*

but not *Pparg1* in the liver (Vidal-Puig et al., 1996; Zhang et al., 2006). Moreover, PPARγ

was reported to be essential for up-regulation of *Scd1* in the liver (Morán-Salvador et al.,

2011). In addition, liver-specific PPARγ knockout has been reported to decrease *Scd1*

expression in AZIP mice, in which *Pparg2* expression is markedly enhanced (Gavrilova

et al., 2003). Furthermore, in null PPARγ knockout mice, the expressions of *Scd1* and

Elovl6 were found to be decreased in adipose tissues that abundantly express PPARγ2 (Virtue et al., 2012). Taken together, HFD-induced upregulation of *Pparg2* via Gpr52 is suggested to be involved in the increase in expressions of *Scd1* and *Elovl6* in the liver of WT mice (Figure 5). Considering that gene ablation of *Acc2* mice was reported to be resistant to HFD-induced heptostatosis (Abu-Elheiga et al., 2012), the lack of induction of *Acc2* by HFD in *Gpr52*$^{-/-}$ mice may well contribute at least in part to their reduced triglyceride accumulation by HFD.

GPR52 was initially cloned from the genomic database (Sawzdargo et al., 1999) and was later found to be expressed abundantly in the brain (Komatsu et al., 2014; Yao et al., 2015). In addition, Nishiyama *et al.* reported that *Gpr52*$^{-/-}$ mice exhibit hyperlocomotion when exposed to a novel environment or when treated by an adenosine A2A receptor (ADORA2A) agonist (Nishiyama et al., 2017), suggesting that the reduced adiposity and enhanced insulin sensitivity of our *Gpr52*$^{-/-}$ mice may be attributable to Gpr52 dysfunction in the brain.

Our present study shows that GPR52 in hepatocytes promotes biosynthesis of fatty acid and cholesterol in a ligand-dependent and a constitutive manner, respectively. The endogenous ligand for GPR52 remains unknown so far, but some members of the fatty acid family might well act as cognate ligands for GPR52, according to sequence-structure

based phylogeny (Kakarala and Jamil, 2014).

It is advantageous for all mammalians to deposit triglyceride in their tissues in case of surplus energy intake. However, in modern human society, excessive fat intake that occurs on a regular basis results in the development of hepatosteatosis and its consequent insulin resistance. Accordingly, compounds that inhibit ligand-dependent GPR52 activation may represent novel therapeutic tools to prevent hepatosteatosis and insulin resistance induced by excessive fat intake in humans.

LIMITATIONS OF THE STUDY

Although we identified that Gpr52 is essential for HFD-induced increase in hepatic expressions of *Pparg2, Scd1,* and *Elovl6*, it remains unknown whether HFD-induced increase of *Scd1* and *Elovl6* is mediated through increased PPARγ2 signaling. In addition, our present study suggests that HFD-derived dietary molecules may activate GPR52 signaling to increase fatty acid biosynthesis in liver. However, the endogenous ligand for GPR52 was not identified in the present study. Furthermore, we could not clarify the regulatory mechanism of cholesterol biosynthesis by GPR52 in liver. Analyses with biased pharmacological ligands and/or blockade of intervening signaling will be helpful to decipher these molecular mechanisms in the future.

AUTHOR CONTRIBUTIONS

Conceptualization, M.W., K.Y., H.O., Y.Y., E.L. and T.Miki; Methodology, M.W., K.Y., and H.O.; Investigation, M.W., K.Y., H.O., K.S., T.Maekawa, and E.L.; Writing - Original Draft, M.W.; Writing - Review & Editing, M.W., T.O., E.L., and T.Miki; Supervision, E.L., and T.Miki.

ACKNOWLEDGMENTS

DECLARATION OF INTERESTS

The authors declare no competing interests.

RESOURCE AVAILABILITY

Lead Contact

Further requests for resources should be directed to the lead contact, Mitsuo Wada (mitsuo.wada @jt.com).

Materials Availability

This work did not generate new unique reagents.

Data and Code Availability

This article includes all analyzed data.

METHODS

All methods can be found in the Transparent Methods supplemental file.

SUPPLEMENTAL INFORMATION

Supplemental Information can be found in the supplemental file.

REFERENCES

Abu-Elheiga, L., Wu, H., Gu, Z., Bressler, R., and Wakil, S.J. (2012). Acetyl-CoA Carboxylase 2−/− Mutant Mice are Protected against Fatty Liver under High-fat, High-carbohydrate Dietary and de Novo Lipogenic Conditions. J. Biol. Chem. *287*, 12578–12588.

ALJohani, A.M., Syed, D.N., and Ntambi, J.M. (2017). Insights into Stearoyl-CoA Desaturase-1 Regulation of Systemic Metabolism. Trends in Endocrinology and Metabolism *28*, 831–842.

Allen, J.A., Raval, S.R., Yang, R., and Xi, S. (2017). Genome-wide tissue transcriptome profiling and ligand screening identify seven striatum-specific human orphan GPCRs. The FASEB Journal *31*, 576.

Bathaie, S.Z., Ashrafi, M., Azizian, M., and Tamanoi, F. (2017). Mevalonate Pathway and Human Cancers. Curr. Mol. Pharmacol. *10*, 77–85.

Chan, M.-Y., Zhao, Y., and Heng, C.-K. (2008). Sequential Responses to High-fat and High-calorie Feeding in an Obese Mouse Model. Obesity *16*, 972–978.

Dobrzyn, P., Jazurek, M., and Dobrzyn, A. (2010). Stearoyl-CoA desaturase and insulin signaling - What is the molecular switch? Biochimica et Biophysica Acta - Bioenergetics *1797*, 1189–1194.

Gavrilova O, Haluzik M, Matsusue K, Cutson JJ, Johnson L, Dietz KR, Nicol CJ, Vinson C, Gonzalez FJ, Reitman ML. (2003). Liver peroxisome proliferator-activated receptor gamma contributes to hepatic steatosis, triglyceride clearance, and regulation of body fat mass. J. Biol. Chem. *278*, 34268-34276.

Guillou, H., Zadravec, D., Martin, P.G.P., and Jacobsson, A. (2010). The key roles of elongases and desaturases in mammalian fatty acid metabolism: Insights from transgenic mice. Progress in Lipid Research *49*, 186–199.

Gusach, A., Maslov, I., Luginina, A., Borshchevskiy, V., Mishin, A., and Cherezov, V. (2020). Beyond structure: emerging approaches to study GPCR dynamics. Current Opinion in Structural Biology *63*, 18–25.

Hatzipantelis, C.J., Lu, Y., Spark, D.L., Langmead, C.J., and Stewart, G.D. (2020). A β-arrestin-2-dependent mechanism of GPR52 signalling in frontal cortical neurons. ACS Chemical Neuroscience.

Hilger, D., Masureel, M., and Kobilka, B.K. (2018). Structure and dynamics of GPCR signaling complexes. Nature Structural and Molecular Biology *25*, 4–12.

Hu, C.C., Qing, K., and Chen, Y. (2004). Diet-induced changes in stearoyl-CoA desaturase 1 expression in obesity-prone and -resistant mice. Obesity Research *12*, 1264–1270.

Hu, S., Liu, K., Luo, H., Xu, D., Chen, L., Zhang, L., and Wang, H. (2019). Caffeine programs hepatic SIRT1-related cholesterol synthesis and hypercholesterolemia via A2AR/cAMP/PKA pathway in adult male offspring rats. Toxicology *418*, 11–21.

Kakarala, K.K., and Jamil, K. (2014). Sequence-structure based phylogeny of GPCR Class A Rhodopsin receptors. Molecular Phylogenetics and Evolution *74*, 66–96.

Khan, A.A., Agarwal, H., Reddy, S.S., Arige, V., Natarajan, B., Gupta, V., Kalyani, A., Barthwal, M.K., and Mahapatra, N.R. (2020). MicroRNA 27a Is a Key Modulator of Cholesterol Biosynthesis. Molecular and Cellular Biology *40*.

Kim, C.W., Addy, C., Kusunoki, J., Anderson, N.N., Deja, S., Fu, X., Burgess, S.C., Li, C., Chakravarthy, M., Previs, S., et al. (2017). Acetyl CoA Carboxylase Inhibition Reduces Hepatic Steatosis but Elevates Plasma Triglycerides in Mice and Humans: A Bedside to Bench Investigation. Cell Metabolism *26*, 394-406.e6.

Komatsu, H., Maruyama, M., Yao, S., Shinohara, T., Sakuma, K., Imaichi, S., Chikatsu, T., Kuniyeda, K., Siu, F.K., Peng, L.S., et al. (2014). Anatomical Transcriptome of G Protein-Coupled Receptors Leads to the Identification of a Novel Therapeutic Candidate GPR52 for Psychiatric Disorders. PLoS ONE *9*, e90134.

Lin, X., Li, M., Wang, N., Wu, Y., Luo, Z., Guo, S., Han, G.W., Li, S., Yue, Y., Wei, X., et al. (2020). Structural basis of ligand recognition and self-activation of orphan GPR52. Nature *579*, 152–157.

Luo, J., Yang, H., and Song, B.L. (2020). Mechanisms and regulation of cholesterol homeostasis. Nature Reviews Molecular Cell Biology *21*, 225–245.

Mao, J., DeMayo, F.J., Li, H., Abu-Elheiga, L., Gu, Z., Shaikenov, T.E., Kordari, P., Chirala, S.S., Heird, W.C., and Wakil, S.J. (2006). Liver-specific deletion of acetyl-CoA carboxylase 1 reduces hepatic triglyceride accumulation without affecting glucose homeostasis. Proceedings of the National Academy of Sciences of the United States of America *103*, 8552–8557.

Martin, A.L., Steurer, M.A., and Aronstam, R.S. (2015). Constitutive Activity among Orphan Class-A G Protein Coupled Receptors. PLOS ONE *10*, e0138463.

Matsuzaka, T., Shimano, H., Yahagi, N., Kato, T., Atsumi, A., Yamamoto, T., Inoue, N., Ishikawa, M., Okada, S., Ishigaki, N., et al. (2007). Crucial role of a long-chain fatty acid elongase, Elovl6, in obesity-induced insulin resistance. Nature Medicine *13*, 1193–1202.

Mauvoisin, D., and Mounier, C. (2011). Hormonal and nutritional regulation of SCD1 gene expression. Biochimie *93*, 78-86.

Morán-Salvador, E., López-Parra, M., García-Alonso, V., Titos, E., Martínez-Clemente, M., González-Périz, A., López-Vicario, C., Barak, Y., Arroyo, V., and Clària, J. (2011). Role for PPARγ in obesity-induced hepatic steatosis as determined by hepatocyte- and macrophage-specific conditional knockouts. FASEB journal : official publication of the Federation of American Societies for Experimental Biology *25*, 2538-2550.

Nakahata, T., Tokumaru, K., Ito, Y., Ishii, N., Setoh, M., Shimizu, Y., Harasawa, T., Aoyama, K., Hamada, T., Kori, M., et al. (2018). Design and synthesis of 1-(1-benzothiophen-7-yl)-1H-pyrazole, a novel series of G protein-coupled receptor 52

(GPR52) agonists. Bioorganic and Medicinal Chemistry *26*, 1598–1608.

Nishiyama, K., Suzuki, H., Maruyama, M., Yoshihara, T., and Ohta, H. (2017). Genetic deletion of GPR52 enhances the locomotor-stimulating effect of an adenosine A2A receptor antagonist in mice: A potential role of GPR52 in the function of striatopallidal neurons. Brain Research *1670*, 24–31.

Ntambi, J.M., Miyazaki, M., Stoehr, J.P., Lan, H., Kendziorski, C.M., Yandell, B.S., Song, Y., Cohen, P., Friedman, J.M., and Attie, A.D. (2002). Loss of stearoyl-CoA desaturase-1 function protects mice against adiposity. Proceedings of the National Academy of Sciences of the United States of America *99*, 11482–11486.

Oosterveer, M.H., van Dijk, T.H., Tietge, U.J.F., Boer, T., Havinga, R., Stellaard, F., Groen, A.K., Kuipers, F., and Reijngoud, D.-J. (2009). High Fat Feeding Induces Hepatic Fatty Acid Elongation in Mice. PLoS ONE *4*, e6066.

Osborn, O., Oh, D.Y., McNelis, J., Sanchez-Alavez, M., Talukdar, S., Lu, M., Li, P.P., Thiede, L., Morinaga, H., Kim, J.J., et al. (2012). G protein-coupled receptor 21 deletion improves insulin sensitivity in diet-induced obese mice. Journal of Clinical Investigation *122*, 2444–2453.

Ritter, S.L., and Hall, R.A. (2009). Fine-tuning of GPCR activity by receptor-interacting proteins. Nature Reviews Molecular Cell Biology *10*, 819–830.

Sawzdargo, M., Nguyen, T., Lee, D.K., Lynch, K.R., Cheng, R., Heng, H.H.Q., George, S.R., and O'Dowd, B.F. (1999). Identification and cloning of three novel human G protein-coupled receptor genes GPR52, ΨGPR53 and GPR55: GPR55 is extensively expressed in human brain. Molecular Brain Research *64*, 193–198.

Setoh, M., Ishii, N., Kono, M., Miyanohana, Y., Shiraishi, E., Harasawa, T., Ota, H., Odani, T., Kanzaki, N., Aoyama, K., et al. (2014). Discovery of the first potent and orally available agonist of the orphan G-protein-coupled receptor 52. Journal of Medicinal Chemistry *57*, 5226–5237.

Shimano, H. (2012). Novel qualitative aspects of tissue fatty acids related to metabolic regulation: Lessons from Elovl6 knockout. Progress in Lipid Research *51*, 267–271.

Tian, L., Song, Y., Xing, M., Zhang, W., Ning, G., Li, X., Yu, C., Qin, C., Liu, J., Tian, X., et al. (2010). A novel role for thyroid-stimulating hormone: Up-regulation of hepatic 3-hydroxy-3-methyl-glutaryl-coenzyme a reductase expression through the cyclic adenosine monophosphate/protein kinase A/cyclic adenosine monophosphate-responsive element binding protein. Hepatology *52*, 1401–1409.

van den Boomen, D.J.H., Volkmar, N., and Lehner, P.J. (2020). Ubiquitin-mediated regulation of sterol homeostasis. Current Opinion in Cell Biology *65*, 103–111.

Virtue, S., Masoodi, M., Velagapudi, V., Tan, C.Y., Dale, M., Suorti, T., Slawik, M.,

Blount, M., Burling, K., Campbell, M., et al. (2012). Lipocalin prostaglandin D synthase and PPARγ2 coordinate to regulate carbohydrate and lipid metabolism in Vivo. PLoS One *7*, 1–12.

Wakil, S.J., and Abu-Elheiga, L.A. (2009). Fatty acid metabolism: Target for metabolic syndrome. Journal of Lipid Research *50*, S138–S143.

Vidal-Puig, A., Jimenez-Liñan, M., Lowell, B.B., Hamann, A., Hu, E., Spiegelman, B., Flier, J.S., and Moller, D.E. (1996). Regulation of PPAR gamma gene expression by nutrition and obesity in rodents. The Journal of clinical investigation *97*, 2553-2561.

Wootten, D., Christopoulos, A., Marti-Solano, M., Babu, M.M., and Sexton, P.M. (2018). Mechanisms of signalling and biased agonism in G protein-coupled receptors. Nature Reviews Molecular Cell Biology *19*, 638–653.

Yao, Y., Cui, X., Al-Ramahi, I., Sun, X., Li, B., Hou, J., Difiglia, M., Palacino, J., Wu, Z.Y., Ma, L., et al. (2015). A striatal-enriched intronic GPCR modulates huntingtin levels and toxicity. ELife *2015*.

Zhang, Y.L., Hernandez-Ono, A., Siri, P., Weisberg, S., Conlon, D., Graham, M.J., Crooke, R.M., Huang, L.S., and Ginsberg, H.N. (2006). Aberrant hepatic expression of PPARgamma2 stimulates hepatic lipogenesis in a mouse model of obesity, insulin resistance, dyslipidemia, and hepatic steatosis. The Journal of biological chemistry *281*, 37603-37615.

FIGURE TITLES AND LEGENDS

Figure 1. *Gpr52$^{-/-}$* Mice Exhibit Leanness Associated with Increased Insulin Sensitivity

(A) Changes in body weight of *Gpr52$^{-/-}$* and WT mice (n = 5). (B) Tissue weight of *Gpr52$^{-/-}$* and WT mice (n = 7, 19 weeks old). (C) OGTT (2 g/kg) in *Gpr52$^{-/-}$* and WT mice. Plasma glucose (left) and insulin (right) concentrations are plotted at the indicated time points (n = 5, 17 weeks old). (D) Representative western blot analysis of p-Akt (S473) level (upper), Akt (middle), and α-tubulin (lower) of epiWAT (left) and liver (right). The

ratio of p-Akt (S473) level to Akt was quantified in the graphs. Data are means ± SEM. *

p <0.05, ** p < 0.01, between the animal groups by unpaired Student's *t*-test.

Figure 2. Gene Expressions of the Enzymes Involved in Biosynthesis of Fatty Acid

and Cholesterol Were Altered in Metabolic Tissues of *Gpr52*^{-/-} Mice

(A) *GPR52* mRNA expression in various human tissues and HepG2 cells. (B) *Gpr52*

mRNA expression in brain, epiWAT, liver, skeletal muscle, and pancreatic islets of mice.

(A, B) Expression levels are shown as relative values normalized to *GAPDH* (A) *or*

Gapdh (B) (n = 3-4). The expressions in brain are represented as 1. (C) *Gpr52* mRNA

expression in adipocyte and SVF in mice. *Adiponectin* (*Adipoq*) and *F4/80* (*Adgre1*) are

indicated as markers of adipocyte and SVF, respectively (n = 4). (D) Gene expressions of

the enzymes involved in fatty acid biosynthesis (*Scd1*, *Elovl6, Acc1*, *Acc2*, *Dgat2*, and

Acss2) and cholesterol biosynthesis (*Hmgcr*) in metabolic tissues (ingWAT, epiWAT, BAT,

and liver) of *Gpr52*^{-/-} and WT mice under fed condition (n = 5, 19 weeks old). Data are

means ± SEM. * p <0.05, ** p < 0.01, between the animal groups by unpaired Student's

t-test.

Figure 3. GPR52 Is Involved in *De novo* Synthesis of Fatty Acid and Cholesterol in

Mice Tissues and a Human Hepatoma Cell Line

(A and B) Thin-layer chromatography (TLC) images of *de novo* synthesis of fatty acid and cholesterol labeled by ^{14}C-acetate in epiWAT (A) and liver (B). The radioactivity (PSL: photostimulated luminescence) of fatty acid and cholesterol in *Gpr52$^{-/-}$* and WT mice (n = 5) (right). Data are means ± SEM. * p <0.05, between the animal groups by unpaired Student's *t*-test. (C) The effect of GPR52 agonist c11 on cAMP production in HepG2 cells treated with GPR52-siRNA or control-siRNA (n = 3). The cAMP levels were normalized by protein concentration. (D) The effect of GPR52 agonist c11 on *de novo* synthesis of fatty acid and cholesterol in HepG2 cells treated with GPR52-siRNA or control-siRNA indicated as TLC image (n = 3). (E, F) The radioactivity (PSL) of fatty acid and cholesterol of TLC image. (G) The effect of GPR52 agonist c11 on gene expressions of fatty acid and cholesterol biosynthesis in HepG2 cells treated with GPR52-siRNA or control-siRNA (n = 3). Data are means ± SEM. $^{\#}$ p <0.05, $^{\#\#}$ p <0.01, vs c11-untreated, control-siRNA-treated cells by unpaired Student's *t*-test. * p <0.05, ** p <0.01, vs control-siRNA-treated, c11-treatment counterparts by unpaired Student's *t*-test.

Figure 4. Gpr52 Accelerates Fat Accumulation in Liver and Induces Insulin Resistance in Response to Excessive Fat Intake

(A) Changes in body weight of *Gpr52*^{-/-} and WT mice in HFD (n = 6-12). (B) Plasma

glucose (left) and insulin (right) concentrations of *Gpr52*^{-/-} and WT mice in fed (n = 8-9)

and fasted (n = 26-39) conditions at 17-18 weeks old. (C) OGTT (2 g/kg) on 17-18 weeks

old *Gpr52*^{-/-} and WT mice. Plasma glucose and insulin concentrations are plotted at the

indicated time points (n = 26-39). (D) Liver weight (left) and hepatic triglyceride content

(right) of *Gpr*52[-/-] and WT mice aged 16-23 weeks under normal diet (ND) (n = 4-6) or

17-week-HFD (n = 15-21). (E) Hepatic gene expressions involved in fatty acid

biosynthesis in *Gpr52*^{-/-} and WT mice fed ND (n = 5) and HFD (n = 9) at 21-23 weeks

old under fed condition. The average Ct value of WT mice fed ND was 22.5, 26.7, 29.0,

27.7, 32.1, and 31.5 for *Scd1*, *Elovl6*, *Acc1*, *Acc2*, *Srebp1c*, and *Pparg2*, respectively,

when cDNAs synthesized from 20 ng of total RNA were used for each qPCR. Data are

means ± SEM. * $p < 0.05$, ** $p < 0.01$, *** $p < 0.001$, between the animal groups by one-

way or two-way analysis of variance (ANOVA) followed by the Tukey-Kramer post-hoc

test.

Figure 5. A Model for HFD-induced Insulin Resistance and Hepatosteatosis via a

GPR52/PPARγ2/lipogenesis Pathway

See text in detail. FA; fatty acid. TG; triglyceride.

Supplementary Figure Legends

Figure S1 (related to Figure 1 and 2). Body Length, Food Intake, Locomotor Activity and Metabolic Phenotype of *Gpr52*$^{-/-}$ Mice

(A) Schematic representation of the *Gpr52*$^{-/-}$ mice. For genotyping *Gpr52*$^{-/-}$ and WT mice, PCR was performed using indicated primer pairs (KEY RESOURCES TABLE). (B) Changes in body length (nose-anus) of *Gpr52*$^{-/-}$ and WT mice (n = 5). (C) Cumulative food intake from 10 to 22 weeks-of-age of *Gpr52*$^{-/-}$ and WT mice (n = 6). (D) Spontaneous locomotor activity of *Gpr52*$^{-/-}$ and WT mice (n = 8, 5-6 weeks old). The changes over time (left) and the total counts (right) are depicted. (E) Plasma glucose (left) and insulin (right) concentrations of *Gpr52*$^{-/-}$ and WT mice in fed conditions (n = 5, 16 weeks old). (F) ITT (0.4 units/kg) on 18 weeks old *Gpr52*$^{-/-}$ and WT mice. Plasma glucose and insulin concentrations are plotted at the indicated time points (n = 5). (B-F) Data are means ± SEM.

Figure S2 (related to Figure 3). Intracellular cAMP Accumulation Activity of GPR52 Agonist c11 and the *GPR52* Was Knocked-down by the siRNA Against GPR52

(A) GPR52 agonist c11 was synthesized in our laboratories in accord with the reported

compound (Nakahata et al., 2018). (B) The effect of c11 on intracellular cAMP accumulation in three types of GloSensor cAMP HEK293 cells, which were transiently transfected with vehicle, GPR52, or GPR21. The cAMP production was measured as luminescence and the data are expressed as fold change relative to c11-untreated, vehicle-expressing HEK293 cells (n = 3). (C) *GPR52* mRNA expression in HepG2 cells treated with GPR52-siRNA or control-siRNA (n = 3). Data are means ± SEM.

Table S1. TaqMan® Primers/probes for qPCR in This Study

Gene	Sequence (5'-3') or assay number
Mouse	
Gapdh	TaqMan® Gene Expression Assay: 4352339E
Adiponectin (Adipoq)	TaqMan® Gene Expression Assay: Mm00456425_m1
F4/80 (Adgre1)	TaqMan® Gene Expression Assay: Mm00802530_m1
Scd1	TaqMan® Gene Expression Assay: Mm00772290_m1
Elovl6	TaqMan® Gene Expression Assay: Mm00851223_s1
Acc1	TaqMan® Gene Expression Assay: Mm01304257_m1

Acc2	TaqMan® Gene Expression Assay: Mm01204659_m1
Dgat2	TaqMan® Gene Expression Assay: Mm00499536_m1
Acss2	TaqMan® Gene Expression Assay: Mm00480101_m1
Hmgcr	TaqMan® Gene Expression Assay: Mm01282499_m1
Srebp1c	Forward: AAGCTGTCGGGGTAGCGTC Reverse: GAGCTGGAGCATGTCTTCAA Probe: FAM- ACCACGGAGCCATGGATTGCACATT-MGB
Pparg2	Forward: GGGTGAAACTCTGGGAGATTCTC Reverse: GATGCCATTCTGGCCCAC Probe: FAM-TGACCCAGAAAGCGATTCCTTCACTGA-MGB
Gpr52	Forward: TTGTCTTGCTGACATTTCTGATCA Reverse: GGAGCACAGTGAAAGACAAAGATG Probe: FAM-CTCTGGGAATTTAAC-MGB
Human	
GAPDH	TaqMan® Gene Expression Assay: 4326317E
SCD1	TaqMan® Gene Expression Assay: Hs01682761_m1
ELOVL6	TaqMan® Gene Expression Assay: Hs00907564
HMGCR	TaqMan® Gene Expression Assay: Hs00168352_m1

GPR52	Forward: CGTTGGAGTTAGCTGCTTGGT
	Reverse: TCGTGGACACCTGTGGAGTAGT
	Probe: FAM-CCTACTCTGTCACTTCT-MGB

Transparent Methods

Mice

Gpr52^{-/-} mice were generated by TRANS GENIC INC. (Kobe, Japan). The targeting vector was constructed so as to replace the entire exon of *Gpr52* with the Neo-cassette (Figure S1). *Gpr52* heterozygous knockout mice (*Gpr52^{+/-}* mice) were generated using the RENKA cell line and were backcrossed over 5 times with C57BL/6J strains. The animals were maintained on CRF-1 (Charles River Laboratories, Inc., Wilmington, MA, USA) as standard laboratory chow diet or high fat diet with 60 kcal% fat (D12492, Research Diets, Inc., New Brunswick, NJ, USA). Entire animal study protocols had been approved by the research institution after a review by the Institutional Animal Care and Use Committee of the Central Pharmaceutical Research Institute, Japan Tobacco Inc.. All animal studies were conducted in accordance with the Japanese Law for the Humane Treatment and Management of Animals.

Cell lines

HepG2 cells were cultured in low glucose (1.5 g/L) Dulbecco's modified Eagle's medium

(DMEM) (Thermo Fisher Scientific, Waltham, MA, USA) supplemented with 10% heat-

inactivated fetal bovine serum (FBS) (Biowest, Kansas City, MO, USA), 1% Penicillin-

Streptomycin (15 mg/mL) (Thermo Fisher Scientific). GloSensor^{TM} cAMP HEK293 cells

were cultured in high glucose (4.5 g/L) Dulbecco's modified Eagle's medium (DMEM)

supplemented with 10% heat-inactivated FBS, 1% Penicillin-Streptomycin, and 0.2

mg/mL hygromycin (Thermo Fisher Scientific).

***in vivo* animal experiments**

All animal studies were conducted using male littermates of *Gpr52$^{-/-}$* and WT mice. Blood

samples were collected from the mice under fed *ad libitum* or overnight (16 hours) fasted

conditions. Plasma glucose, triglyceride, and cholesterol levels were measured by an

enzymatic method (FUJIFILM Wako Pure Chemical Corporation, Osaka, Japan). Plasma

insulin levels were measured by an enzyme-linked immunosorbent assay (Ultra Sensitive

Mouse Insulin ELISA Kit, Morinaga Institute of Biological Science, Yokohama, Japan).

Spontaneous locomotor activity of mice was assessed using a Supermex apparatus

(Muromachi Kikai Co., Ltd., Tokyo, Japan). An infrared beam sensor was placed on top

of an acrylic cage. Mice were placed individually into the cage and the number of movements over two days was counted in 60-minute bins. Mice had free access to food and water during measurements.

To assess glucose tolerance, the mice were fasted overnight (approximately 16 hours) and glucose (2 g/kg body weight, Nacalai tesque, Kyoto, Japan) was administered orally. To assess insulin tolerance, the mice were fasted overnight (approximately 16 hours) and insulin (0.4 units/kg body weight, Novo Nordisk A/S, Bagsværd, Denmark) was injected intraperitoneally.

For measuring hepatic triglyceride content, the liver was collected from the mice euthanized at fed state and a portion of the liver (about 100 mg) was excised and lysed with methanol using a mixer mill (Retsch MM300, Verder Scientific Co., Ltd., Haan, Germany) at 25Hz for 10 min. Chloroform was added to the homogenized solution and mixed thoroughly. After centrifugation, the supernatant was collected. The solution of lipid extracts was dried under a stream of nitrogen gas. 2-propanol was added to the dried lipid extracts and the triglyceride content was determined by an enzymatic method.

in vitro cell line experiments

HepG2 cells (ATCC) were cultured in DMEM (low glucose), 10% FBS, and 1% Penicillin-Streptomycin (growth medium). For siRNA experiments of GPR52, HepG2 cells were seeded in 24 well-plate at 1.5×10^5 cells/well. The following day, 20 nM siRNA for GPR52 (Thermo Fisher Scientific) was transfected using Lipofectamine$^®$ RNAiMax (Thermo Fisher Scientific) and the cells were incubated another two days. The medium was replaced with growth medium and incubated with each concentration of GPR52 agonist for 15 hours, and the cells were then subjected to quantitative RT-PCR and *de novo* lipogenesis assay. To evaluate the effect of c11 on cAMP production, the cells were pre-incubated in serum-free medium containing 0.5 mM 3-isobutyl-1-methylxanthine (IBMX, Merck KGaA, Darmstadt, Germany) for 30 min followed by stimulation with a differing concentration of c11. After 1 hour incubation, the cells were lysed and the cAMP concentration was measured by an enzyme-linked immunosorbent assay (Direct cAMP ELISA kit, Enzo Biochem Inc., New York, NY, USA). The GPR52 agonist c11 was synthesized at Central Pharmaceutical Research Institute, Japan Tobacco Inc. (Osaka, Japan).

HEK293 cells stably expressing pGloSensor^{TM}-22F cAMP were obtained from Promega Corporation (Madison, WI, USA) and cultured in DMEM (high glucose) supplemented by 10% FBS, 1% Penicillin-Streptomycin, and 0.2 mg/mL hygromycin.

The cells were seeded in 96 well-plate at 0.3×10^5 cells/well. The following day, each expression plasmid (pME18S, pME18S-human GPR52, or pME18S-human GPR21) was transfected using Lipofectamine® 2000 (Thermo Fisher Scientific) and the cells were incubated another day. The cells were equilibrated with GloSensor™ cAMP reagent (Promega Corporation) for 2 hours, and then treated with a different concentration of GPR52 agonist c11 for another 6 hours. Intracellular cAMP production was measured by luminescence with GloMax-Multi Detection System (Promega Corporation).

For measuring *de novo* lipid synthesis, HepG2 cells were labeled with 0.25 μCi/mL [^{14}C] acetate (Moravek Biochemicals, Brea, CA, USA) for 2 hours as previously reported (Lee et al., 2017; Okuma et al., 2015). At the end of incubation, the medium was removed and the cells were washed with PBS. Total lipids were extracted 2 times with hexane/isopropanol (3:2). The lipids extracts were dried under a stream of nitrogen gas and reconstituted in methanol. Total lipids were saponified with 1N NaOH (60 min, 70°C) and neutralized with HCl. After saponification, lipids were re-extracted with chloroform and separated via TLC using a hexane/diethylether/acetic acid (80:20:1) solvent system. The radioactivity of each band on a TLC plate was measured as photostimulated luminescence (PSL) with BAS3000 imaging system (FUJIFILM Corporation, Tokyo, Japan).

ex vivo animal experiments

For *ex vivo* lipogenesis assay, epidydimal white adipose tissue (epiWAT) and liver were collected from mice euthanized at fed state, and a portion of the liver (~ 100 mg) was added to the reaction buffer (120 mM NaCl, 4.7 mM KCl, 1.2 mM KH_2PO_4, 2.5 mM $CaCl_2$, 1.2 mM $MgCl_2$, 10 mM HEPES, pH 7.4, 5.5 mM Glucose, 0.25 µCi/mL [^{14}C] acetate) and incubated for 60 min at 37°C. After incubation, total lipids were extracted using chloroform/methanol (2:1) solvent and the equivalent lipid extract of the same tissue weight was separated via TLC. The radioactivity of each band was measured in the same manner as that described above.

For isolating the adipocyte and SVF, portions of mice epidydimal adipose tissues were digested with collagenase type I (Nitta Gelatin, Osaka, Japan) in Krebs Ringer Bicarbonate HEPES (KRBH) buffer (120 mM NaCl, 4 mM KH_2PO_4, 1 mM $MgSO_4$, 1 mM $CaCl_2$, 10 mM $NaHCO_3$, 30 mM HEPES, pH7.4, 20 µM adenosine, 1% BSA) for up to 60 min at 37°C, as previously reported (Yu et al., 2011). Adipocyte suspensions were filtered through nylon mesh and centrifuged at 210g for 1 minute. The floating fraction was collected and washed with KRBH to purify the mature adipocyte. The pellets

containing the SVF were washed with KRBH to remove residual collagenase and adipocyte.

RNA extraction and quantitative RT-PCR

Total RNA from mice tissues and cells was isolated using RNeasy lipid Tissue/RNeasy Mini Kit (Qiagen, Hilden, Germany). The same quantity of total RNA was applied to synthesize cDNA using ReverTra Ace cDNA transcription kit (TOYOBO CO., LTD., Osaka, Japan). Quantitative PCR was performed on ABI7900 using TaqMan™ Gene Expression Master Mix (Thermo Fisher Scientific) with the following cycle parameters: 1 cycle of 50°C for 2 min and 95°C for 10 min, followed by 40 cycles of 95°C for 15 sec and 60°C for 1min. The TaqMan® primers/probes used are shown in Table. S1.

Western blotting

The mice were injected with 0.025 units/kg insulin intravenously and then epiWAT and liver were removed five minutes afterward and then immediately frozen in liquid N_2. The tissues were lysed in 1× RIPA buffer (Cell Signaling Technology, Inc., Danvers, MA, USA) with protease inhibitor cocktail and phosphatase inhibitor cocktail (Cell Signaling Technology, Inc.). Twenty μg protein for epiWAT and 50 μg protein for liver was

subjected to SDS-PAGE. Antibodies against the following proteins were used: phospho-Akt (p-S473) (1:1000) (Cell Signaling Technology, Inc.), α-tubulin (1:1000) (Santa Cruz Biotechnology, Dallas, TX, USA). Band intensity was determined by the LAS-3000 Image Gauge W software (FUJIFILM Corporation) according to the manufacturer's instructions.

Quantification and Statistical Analysis

Results were expressed as means ± SEM. The statistical significances between the samples were determined by the unpaired Student's t-test or a one-way or two-way analysis of variance (ANOVA) followed by the Tukey–Kramer post-hoc test. $p < 0.05$ was considered significant.

KEY RESOURCES TABLE

REAGENT or RESOURCE	SOURCE	IDENTIFIER
Antibodies		
Rabbit anti-phospho-Akt (p-S473) antibody	Cell Signaling Technology, Inc.	Cat# 4060
Rabbit anti-Akt antibody	Cell Signaling Technology, Inc.	Cat# 4691
Mouse anti-α-tubulin antibody	Santa Cruz Biotechnology	Cat# sc-5286
Biological Samples		
Human MTC (Multiple Tissue cDNA) cDNA Panels I	Takara Bio USA, Inc.	Cat# 636742
Human MTC (Multiple Tissue cDNA) cDNA Panels II	Takara Bio USA, Inc.	Cat# 636743
Human Adipose Tissue Total RNA	Takara Bio USA, Inc.	Cat# 636558

Chemicals, Peptides, and Recombinant Proteins		
Novolin R 100IU/mL	Novo Nordisk A/S	N/A
D-(+)-Glucose	Nacalai tesque	Cat# 16805-35
QIAzol Lysis Reagent	Qiagen	Cat# 79306
Acetic acid, sodium salt, [2-^{14}C]/Sodium acetate	Moravek Biochemicals	Cat# MC-213
RIPA Buffer (10X)	Cell Signaling Technology, Inc.	Cat# 9806
Protease Inhibitor Cocktail (100X)	Cell Signaling Technology, Inc.	Cat# 5871
Phosphatase Inhibitor Cocktail (100X)	Cell Signaling Technology, Inc.	Cat# 5870
Hexane	Junsei Chemical Co., Ltd.	Cat# 67150-3130
Isopropanol	Junsei Chemical Co., Ltd.	Cat# 64605-3230
methanol	Junsei Chemical Co., Ltd.	Cat# 73125-2580
diethylether	Junsei Chemical Co., Ltd.	Cat# 33475-3630
acetic acid	Junsei Chemical Co., Ltd.	Cat# 31010-3130
chloroform	Junsei Chemical Co., Ltd.	Cat# 28560-3080
DMEM, low glucose	Thermo Fisher Scientific	Cat# 11885084
DMEM, high glucose	Thermo Fisher Scientific	Cat# 11995065
Penicillin-Streptomycin	Thermo Fisher Scientific	Cat# 15070063
Hygromycin B	Thermo Fisher Scientific	Cat# 10687010
Fetal bovine serum	Biowest	Cat# S1810
3-Isobutyl-1-methylxanthine (IBMX)	Merck KGaA	Cat# I5879
BSA solution 30% in saline, fatty acid free	Merck KGaA	Cat# A9205
Collagenase L	Nitta Gelatin	N/A
Critical Commercial Assays		
Glucose CII test WAKO	FUJIFILM Wako Pure Chemical Corporation	Cat# 439－90901
Cholesterol E test WAKO	FUJIFILM Wako Pure Chemical Corporation	Cat# 439－17501
Triglyceride E test WAKO	FUJIFILM Wako Pure Chemical Corporation	Cat# 432－40201
Ultra Sensitive Mouse Insulin ELISA Kit	Morinaga Institute of Biological Science, Inc.	Cat# 49170-54
GloSensor cAMP Reagent	Promega Corporation	Cat# E1290
RNeasy Mini Kit	Qiagen	Cat# 74106
RNeasy lipid Tissue Mini Kit	Qiagen	Cat# 74804
ReverTra Ace qPCR RT Kit	TOYOBO CO., LTD.	Cat# FSQ-101

TaqMan™ Gene Expression Master Mix	Thermo Fisher Scientific	Cat# 4369016
Lipofectamine® RNAiMAX Transfection Reagent	Thermo Fisher Scientific	Cat# 13778075
Lipofectamine® 2000 Transfection Reagent	Thermo Fisher Scientific	Cat# 11668019
Direct cAMP ELISA kit	Enzo Life Sciences, Inc.	Cat# ADI-900-066
Experimental Models: Cell Lines		
HepG2 cells	ATCC	Cat# HB-8065
GloSensor™ cAMP HEK293 Cell Line	Promega Corporation	Cat# E1261
Experimental Models: Organisms/Strains		
Gpr52−/− mice	TRANS GENIC INC.	N/A
C57BL/6J mice	Charles River Laboratories, Inc.	N/A
Oligonucleotides		
Genotyping DNA primer for endogenous *Gpr52* allele (forward) GAAAGTTCTCGTGTCTTGGACA	Thermo Fisher Scientific	N/A
Genotyping DNA primer for endogenous *Gpr52* allele (reverse) ATGCTGGTAAGGCTGGGCTTAAC	Thermo Fisher Scientific	N/A
Genotyping DNA primer for mutant allele (forward) AGAACAGTCTGTAGTCCTCAC	Thermo Fisher Scientific	N/A
Genotyping DNA primer for mutant allele (reverse)AGGTGAGATGACAGGAGATC	Thermo Fisher Scientific	N/A
TaqMan® primers/probes (Table S1)	Thermo Fisher Scientific	N/A
Silencer Select Negative Control No. 1 siRNA	Thermo Fisher Scientific	Cat# 4390844
siRNA for human GPR52	Thermo Fisher Scientific	Cat# s17764
Recombinant DNA		
pME18S vector	Provided by Dr. K. Maruyama	N/A
Software and Algorithms		
Image Gauge W	FUJIFILM Corporation	N/A
Other		
Supermex apparatus	Muromachi Kikai Co., Ltd.	N/A
Retsch MM300	Verder Scientific Co., Ltd.	N/A
BAS3000 imaging system	FUJIFILM Corporation	N/A
Applied Biosystems 7900HT Fast Real-Time PCR System	Thermo Fisher Scientific	N/A
LAS-3000 Imaging system	FUJIFILM Corporation	N/A
NanoDrop ND-1000	Thermo Fisher Scientific	N/A
GloMax-Multi Detection System	Promega Corporation	N/A

Supplementary References

Yu, G., Floyd, Z.E., Wu, X., Halvorsen, Y.D.C., and Gimble, J.M. (2011). Isolation of human adipose-derived stem cells from lipoaspirates. Methods in Molecular Biology (Clifton, N.J.) *702*, 17–27.

Lee, G., Zheng, Y., Cho, S., Jang, C., England, C., Dempsey, J.M., Yu, Y., Liu, X., He, L., Cavaliere, P.M., et al. (2017). Post-transcriptional Regulation of De Novo Lipogenesis by mTORC1-S6K1-SRPK2 Signaling. Cell *171*, 1545-1558.e18.

Okuma, C., Ohta, T., Tadaki, H., Ishigure, T., Sakata, S., Taniuchi, H., Sano, R., Hamada, H., Kume, S., Nishiu, J., et al. (2015). JTP-103237, a monoacylglycerol acyltransferase inhibitor, prevents fatty liver and suppresses both triglyceride synthesis and de novo lipogenesis. Journal of Pharmacological Sciences *128*, 150–157.
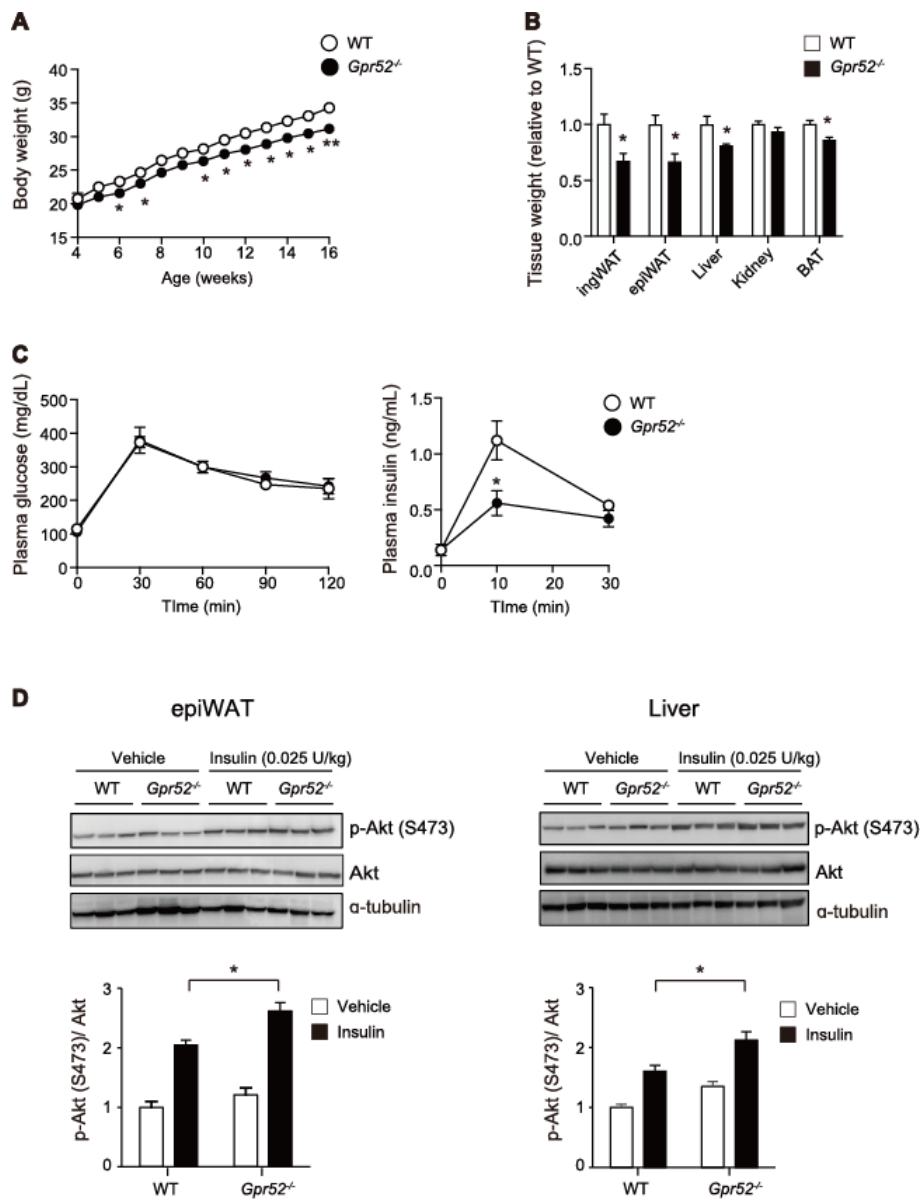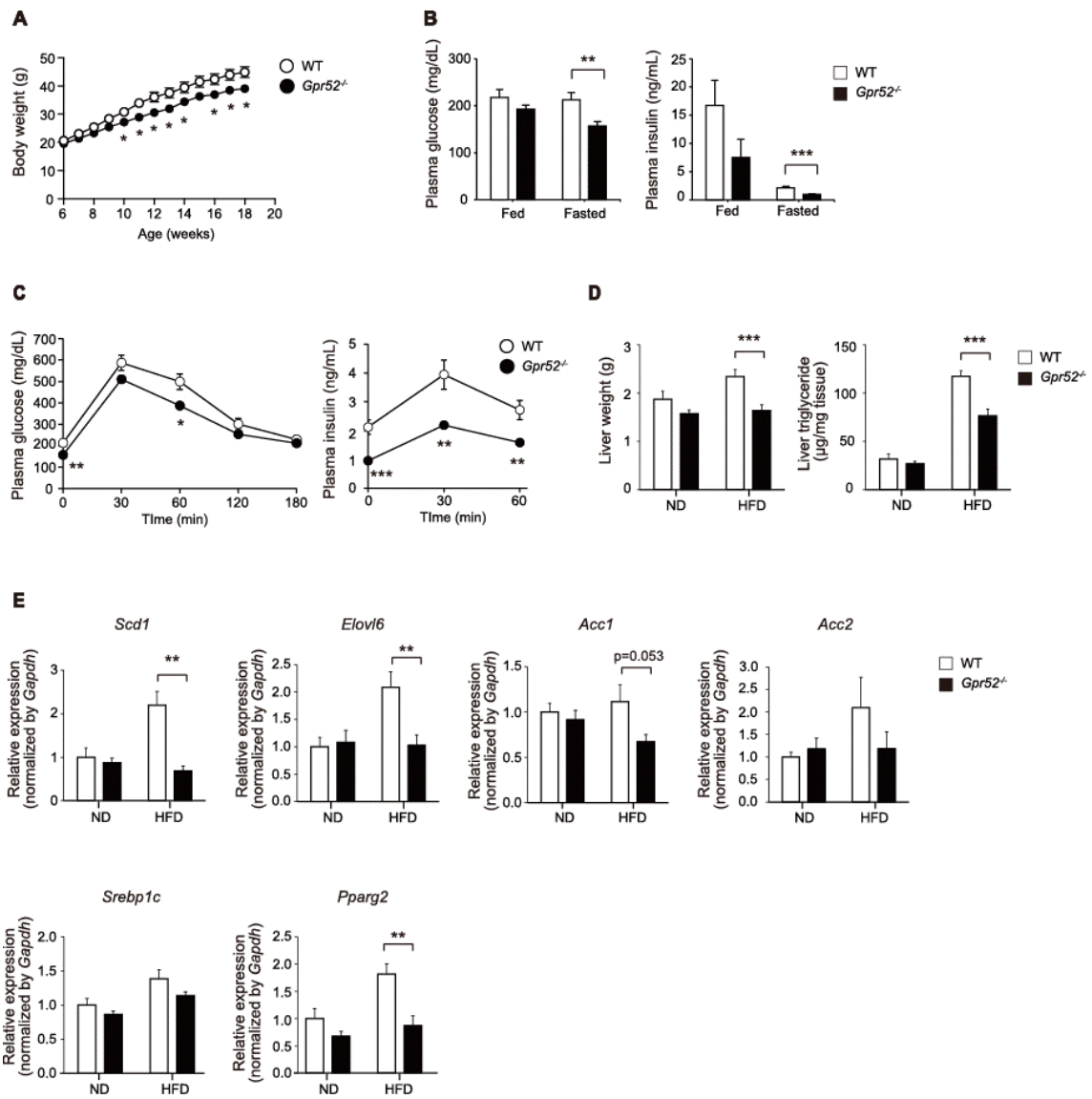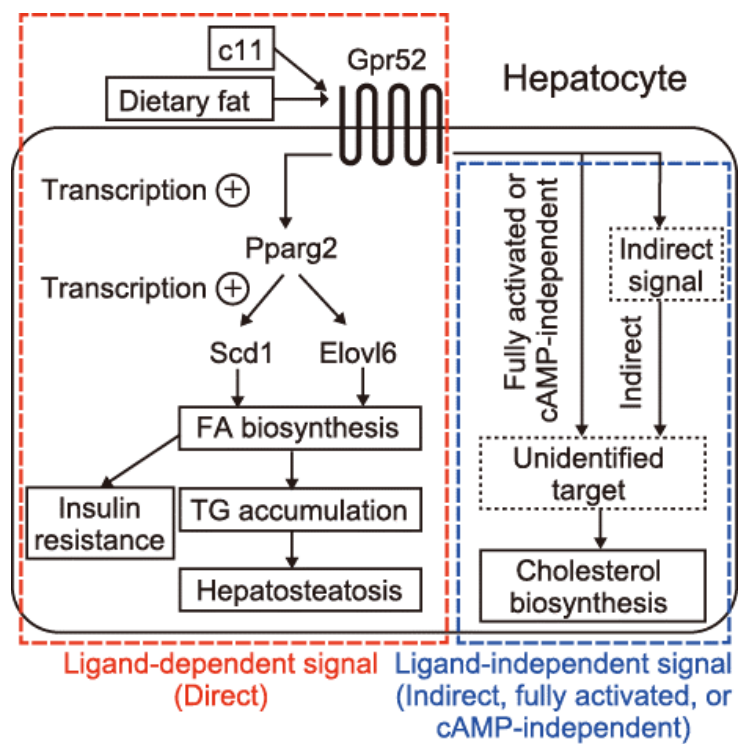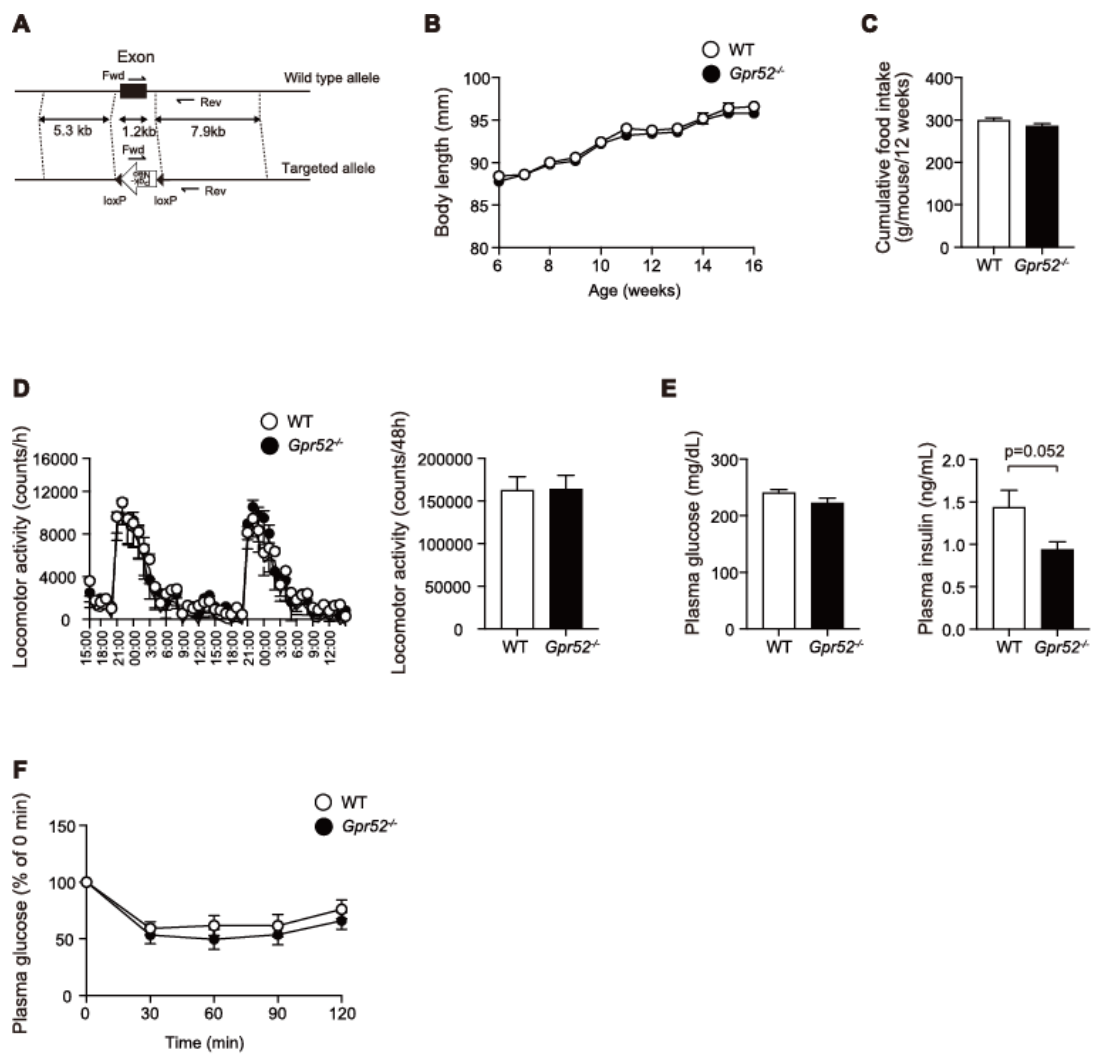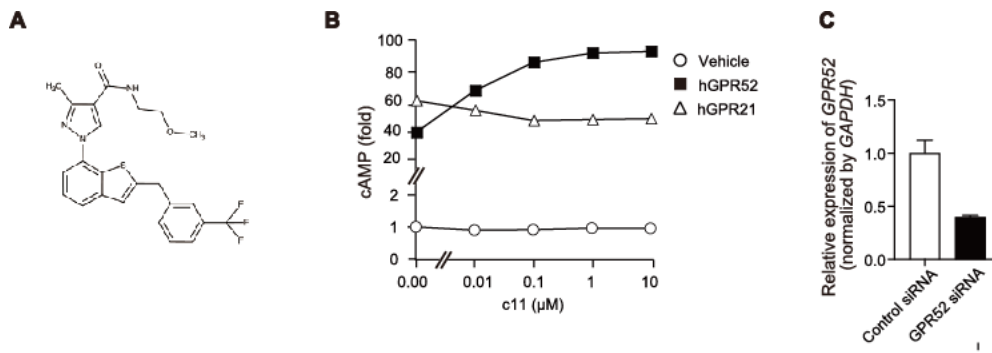
Figure 1.
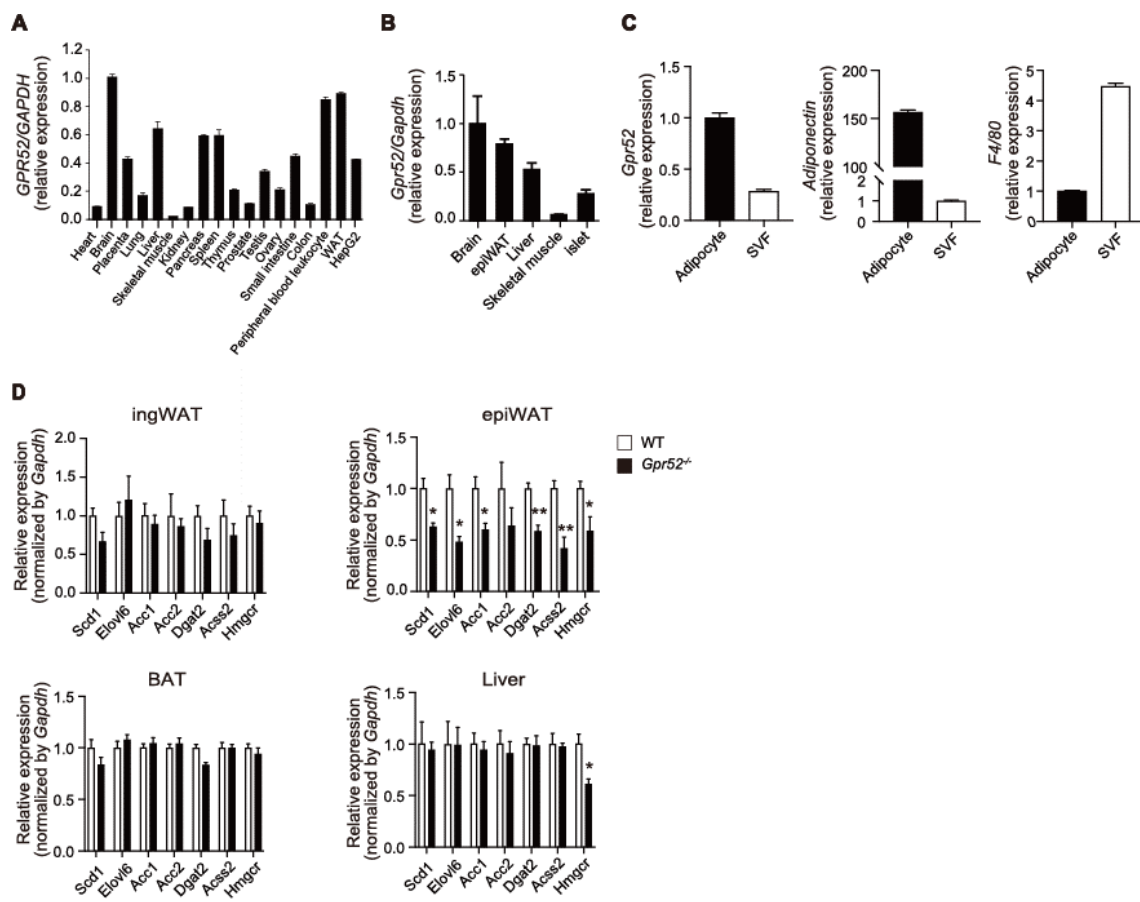
Figure 2.
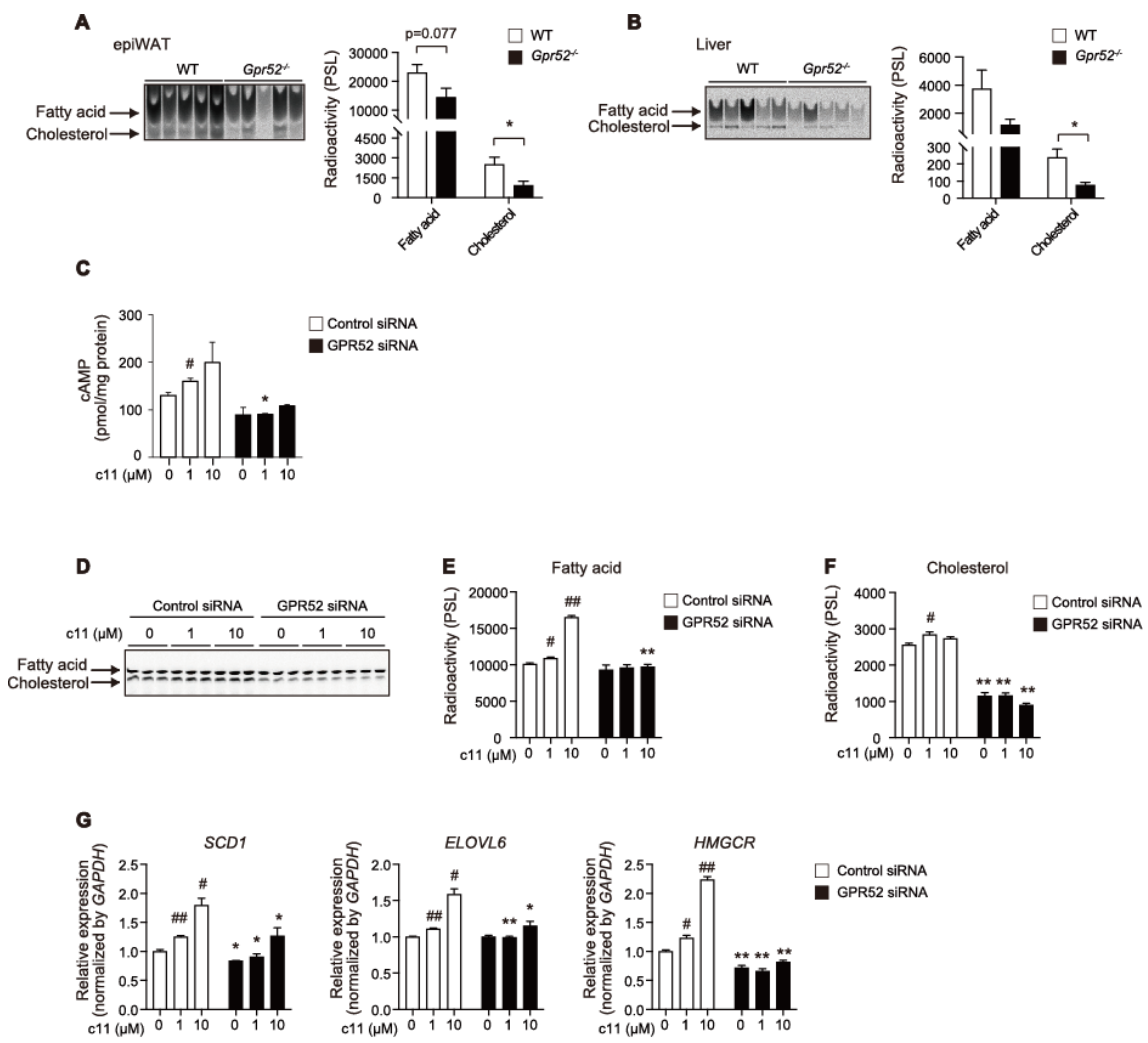
Figure 3.

Figure 4.

Figure 5.

Figure S1.

Figure S2.